Multiple magnetic phase transitions in $PrCoAl_4$ Observed by Muon Spin Rotation and Relaxation Measurements

A. Schenck and F. N. Gygax
Institute for Particle Physics of ETH Zürich (IPP), CH-5232 Villigen PSI, Switzerland

P. Schobinger-Papamantellos
Laboratorium für Kristallographie, ETH Hönggerberg, CH-8093 Zürich, Switzerland

L. D. Tung
Department of Physics, University of Warwick, Coventry CV4 7AL, United Kingdom
(Received 11 November 2004; published 14 June 2005)

Zero field muon spin rotation and relaxation (μSR) measurements on a single crystal of orthorhombic $PrCoAl_4$ revealed the presence of spontaneous static fields, extending above the well-known incommensurately modulated antiferromagnetic structure (T_N=17 K) up to at least 110 K. Two further transitions at 30 K and 84 K were clearly visible. The spontaneous fields above T_N are confined to the (b,c) plane and are tentatively ascribed to a spin density wave involving the Co 3*d*-band electrons.

DOI: 10.1103/PhysRevB.71.214411 PACS number(s): 76.60.Jx, 75.30.Kz, 76.75.+i, 75.25.+z

I. INTRODUCTION

The magnetic properties of orthorhombic $PrCoAl_4$ have recently been studied by susceptibility and magnetization,[1] neutron diffraction,[2,3] and specific heat measurements.[4] $PrCoAl_4$ crystallizes in the $LaCoAl_4$-type structure (space group *Pnma*, no. 51) (see Fig. 1). The only other rare-earth-based compounds of this type are $LaCoAl_4$ and $CeCoAl_4$.[5] The orthorhombic crystal electric field (CEF) splits the $^3H_4$ ground state multiplet of Pr^{3+} into nine singlets. The specific heat data point to two closely spaced singlets placed about 135 K above the lowest nonmagnetic singlet state.[4] The susceptibility measurements[1,2] reveal pronounced anisotropies and identify the crystalline *c* axis as the easy axis. The overall behavior of the susceptibility is typical for an enhanced Van Vleck paramagnet. Below 17 K $PrCoAl_4$ shows a sine-wave longitudinal amplitude modulated antiferromagnetic (AF) structure with an almost temperature-independent propagation vector $\boldsymbol{q}=(0,0,0.4087(5))$, as found by neutron diffraction on a single-crystal sample.[2,3] The amplitude of the wave, 2.24(4) μ_B/Pr at 1.5 K, oriented along the *c* axis, is reduced compared to the Pr^{3+} free-ion moment of 3.2 μ_B, pointing to strong crystal-field effects. To find magnetic order in a singlet ground state compound the exchange coupling between neighboring Pr ions has to surpass a certain critical value, comparable to the energy of the first excited CEF level. It is also worth mentioning that at 4.2 K a spin-flop transition is observed in the case that the external field is oriented parallel to the *c* axis and rises above 0.7 T.[4] The neutron work did not show, down to 1.5 K, any evidence for a squaring up of the sine-wave modulation towards a long-period commensurate structure or an equal-amplitude antiphase domain structure, where in the latter case the moments within a block have equal moments, changing sign from one block to the next in the direction of the wave vector.[3]

In order to check the persistence of the incommensurate sine-wave AF structure down to low temperatures by a different technique, a muon spin rotation/relaxation (μSR) study was initiated. This local probe technique has proven to be able to distinguish between commensurate and incommensurate structures quite easily, as shown in the case of CeSi.[6] In this compound the interpretation of neutron-scattering measurements, initially assumed to indicate an incommensurately modulated AF structure,[7] was later revised to agree with the μSR results.[6] However, the results to be presented in this paper reveal completely unexpected magnetic features of $PrCoAl_4$ above $T_N \simeq 17$ K, appearing to show further transitions at 30 K and 84 K, while the μSR signal below 17 K is too complex to allow unambiguous fits (see Sec. III). Hence this paper is mainly concerned with the results obtained above $T_N \simeq 17$ K in zero applied field.

II. EXPERIMENTAL DETAILS

The μSR measurements in the zero applied field (ZF) and some preliminary measurements in the transverse field (TF)

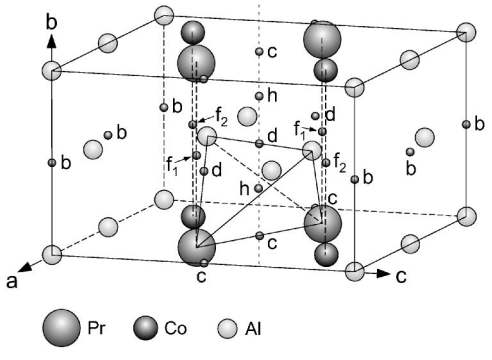

FIG. 1. The crystal structure of orthorhombic $PrCoAl_4$. Indicated are the interstitial sites *b*, *c*, *d*, *h*, f_1 and f_2. The sites f_1 are midway between Pr ions, the sites f_2 midway between Co ions, along the *b* axis. The sites *c*, *d*, *h* are situated in a kind of open channel and may, therefore, not provide deep traps for the μ^+.

of 6 kOe were carried out at the Swiss Muon Source SμS of the Paul Scherrer Institute (PSI), using the general purpose instruments GPS and Dolly on the πM3 and πE3 surface μ^+ beam lines, respectively. The single crystal sample was grown by means of a modified tri-arc Czochralski technique[4] and cut into approximately cubic volume ($1.64\times1.72\times1.78$ mm^3), with the edges along the *a*, *b*, *c* crystal axes. The crystal was mounted in the cryostats of both instruments such that it could be rotated around the *b* axis and the momentum (or beam axis) of the incoming μ^+ was perpendicular to the *b* axis, allowing the initial polarization $\boldsymbol{P}_\mu(0)$ to turn in the (a,c) plane. For the ZF measurements $\boldsymbol{P}_\mu(0)$ was parallel to the beam axis. The positrons from the μ^+ decay could be recorded in forward and backward placed detectors with respect to the beam axis. In the TF measurements the applied field $\boldsymbol{H}_{\rm ext}$ was oriented parallel to the beam axis and $\boldsymbol{P}_\mu(0)$ was rotated by $\sim45°$ from parallel to the beam axis towards the vertical direction by means of a spin rotator placed up stream in the μ^+ beam line πM3. In this case the positrons were recorded in up, down, and right-placed detectors with respect to the beam axis. The cryostats allowed us to set temperatures between 1.8 K and 300 K.

As usual the μSR signal is obtained from the positron rate along direction $\boldsymbol{r}$ $(r=1)$ versus elapsed μ^+ lifetime,[8] i.e.,

$$\frac{dN}{dt} = N_o e^{-t/\tau_\mu}[1 + A\boldsymbol{P}(t)\cdot\boldsymbol{r}], \tag{1}$$

where $\boldsymbol{P}(t)$ describes the evolution of the μ^+ polarization in the sample after implantation, *A* is the effective decay asymmetry of the μ^+ and $\tau_\mu=2.2$ μs the mean μ^+ lifetime. Typically 3–4 million decay events were accumulated per detector.

III. RESULTS

Above T_N the ZF-μSR signal $P(t)$ was best fitted by a sum of three components: a Gaussian-damped precession component, a just Gaussian-damped component, showing no or an extremely slow precession, and an exponentially decaying term, i.e.,

$$P(t) = p_1 \exp\left(-\frac{1}{2}\sigma_1^2 t^2\right)\cos\omega t + p_2 \exp\left(-\frac{1}{2}\sigma_2^2 t^2\right) + p_3 \exp(-\lambda t), \tag{2}$$

with $p_1+p_2+p_3=1$, implying that all μ^+ implanted into the sample contribute to the signal. In the fit of Eq. (1) to the data the decay asymmetry *A* was fixed to a calibrated value. Irrespective of the form of Eq. (2) the data reveal an overall fast relaxation which, as will be discussed further down, can only be understood to arise from magnetic fields of electronic origin.

The amplitudes p_i depend on the orientation of the crystal with respect to the initial $\boldsymbol{P}(0)$. This is demonstrated in Fig. 2 which shows $AP(t)$ at 20 K for $\boldsymbol{P}(0)\|a$ axis and $\boldsymbol{P}(0)\|c$ axis. The fitted orientation dependence of the p_i is displayed in Fig. 3. The solid lines are fits as discussed further down. As can be seen the exponentially damped component is essentially absent for $\boldsymbol{P}(0)\|a$ axis and dominant for $\boldsymbol{P}(0)\|c$ axis. The parameters ω, σ_1, σ_2, and λ are found to be orientation independent; λ is generally rather small (~0.3 μs^{-1}).

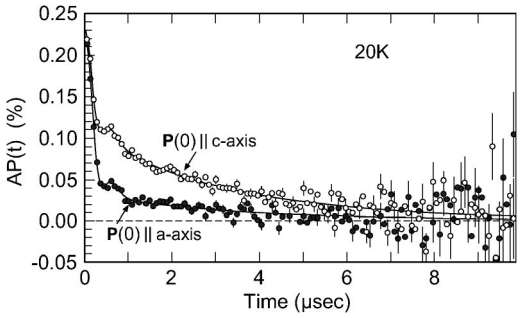

FIG. 2. The ZF signals $AP(t)$ at 20 K for $\boldsymbol{P}(0)$ oriented approximately parallel to the *c*, respectively *a* axis ("backward" e^+ detector). The solid lines are fits of Eq. (2) to the data. Since $\boldsymbol{P}(0)$ was not oriented strictly parallel to the *a* axis a small contribution from the exponentially damped component p_3 is present in this signal.

The first two components reflect the presence of static internal fields $\boldsymbol{B}_{{\rm int},i}$ which cause the μ^+ spin to precess around $\boldsymbol{B}_{{\rm int},i}$. The first term reveals that the average of $|\boldsymbol{B}_{{\rm int},1}|$ is finite and the second term that the average of $|\boldsymbol{B}_{{\rm int},2}|$ is very small, i.e., much smaller than the spread $\Delta\boldsymbol{B}_{{\rm int},2}$, which becomes manifest via the Gaussian decay constant σ_2 ($\Delta B_{{\rm int},i}=\sigma_i/\gamma_\mu$, where $\gamma_\mu=2\pi\times13.55$ krad G^{-1}). The Gaussian decays indicate that the internal field distributions, associated with the two components, are also Gaussian. The third component reveals the presence of additional fluctuating magnetic fields, perpendicular to the static $\boldsymbol{B}_{\rm int}$, which cause the nonprecessing polarization component along $\boldsymbol{B}_{\rm int}$ to relax according to the spin-lattice relaxation mechanism. Since λ is quite small, applying Redfield theory,[9] one deduces that the fluctuations must be either quite fast or of small amplitude. As we did not perform longitudinal field studies it is not possible at present to characterize the fluctuations and say more about their implications.

The fact that the amplitudes p_i are orientation dependent implies that the $\boldsymbol{B}_{{\rm int},i}$ are not randomly oriented but possess a certain preferred direction with respect to the crystal frame. If $\boldsymbol{B}_{\rm int}$ is expressed as $\boldsymbol{B}_{\rm int}=B_{\rm int}(\sin\theta\cos\phi\,\hat{x}, \sin\theta\sin\phi\,\hat{y}, \cos\theta\,\hat{z})$ where $\hat{x}$, $\hat{y}$, $\hat{z}$ are unit vectors along the

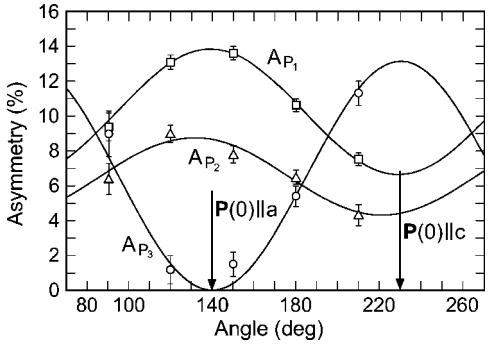

FIG. 3. The orientation dependence of the amplitudes p_1, p_2, and p_3 of the ZF signals at 20 K. The solid lines represent fits of Eq. (3) to p_1 and p_2 and of Eq. (4) to p_3.

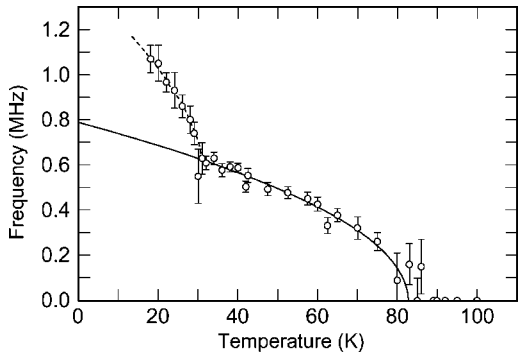

FIG. 4. The temperature dependence of the spontaneous precession frequency $\nu=\omega/2\pi$ [from fits of Eq. (2)]. The solid line represents a fit of Eq. (5) to the data for $T\geqslant 30$ K; the dashed line serves to guide the eye. Note the break at 30 K.

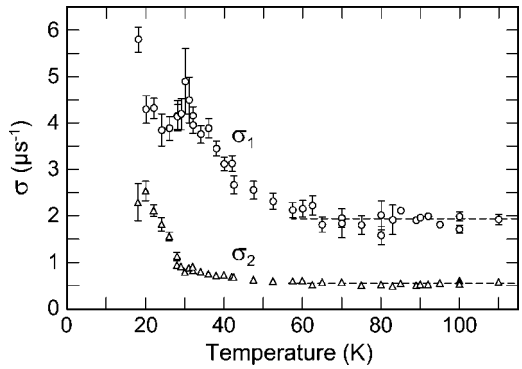

FIG. 5. The temperature dependence of the Gaussian damping constants σ_1 and σ_2 [from fits of Eq. (2)]. Note the anomalies at 30 K, and the temperature independence above ~60 K.

a, c and b crystal axes, the amplitude p_1 (measured in forward or backward direction) is given by the expression[10]

$$p_1 = f_1\left[\left(1-\frac{1}{2}\sin^2\theta_1\right)-\frac{1}{2}\sin^2\theta_1\cos[2(\varphi+\phi_1)]\right], \quad (3)$$

where φ is the angle between the a axis and $\boldsymbol{P}(0)\|$ beam axis. The corresponding line in Fig. 3 represents a fit of Eq. (3) to $p_1(\varphi)$, resulting in $\theta_1=45°\pm2°$ and $\phi_1=90°\pm2.5°$. Hence the average $\boldsymbol{B}_{\mathrm{int},1}$ at 20 K is confined to the (b,c) plane and encloses an angle of 45° with the c axis. However, note that $\sin^2 45°=0.5=(1/\pi)\int_0^\pi \sin^2\theta d\theta$ and hence the same result is obtained for a random orientation of $\boldsymbol{B}_{\mathrm{int},1}$ within the (b,c) plane.

In this respect the second term in Eq. (2) constitutes the 2D analog to the 3D Gaussian Kubo-Toyabe function.[11] The amplitude p_2 can be fitted by Eq. (3) as well (solid line in Fig. 3), yielding $\theta_2=46°\pm4°$ and $\phi_2=95°\pm5°$, essentially equal to θ_1 and ϕ_1, respectively. In this case a random orientation of $\boldsymbol{B}_{\mathrm{int},2}$ in the (b,c) plane at the involved μ^+ site appears most likely.

The amplitude p_3, referring to the polarization component parallel to $\boldsymbol{B}_{\mathrm{int},3}$, is given by the equation[10]

$$p_3 = f_3\tfrac{1}{2}\sin^2\theta_3\{1+\cos[2(\varphi+\phi_3)]\}. \quad (4)$$

The corresponding fit yields $\phi_3=91°\pm2.4°$ with θ_3 fixed at 45° (solid line in Fig. 3), confirming the results from p_1 and p_2. We will come back to a discussion of these results in the next section.

The temperature dependence of $\nu=\omega/2\pi$, σ_1, σ_2, p_1, and p_2 has been measured between 18 K and 100 K for $\boldsymbol{P}(0)\|a$ axis, for which $p_3\simeq 0$. The results are displayed in Figs. 4–6. The observed spontaneous frequency ν drops to zero around 85 K and shows a drastic anomaly at 30 K. The data from 30 K upwards can be well fitted by the phenomenological expression

$$\nu(T)=\nu_0\left[1-\left(\frac{T}{T_{\mathrm{cr}}}\right)^{\delta}\right]^{\beta}, \quad (5)$$

yielding $T_{\mathrm{cr}}=82.7(2.0)$ K with $\delta\equiv 1$ and $\beta\equiv 0.5$ (solid line in Fig. 4). At 18 K $\nu\simeq 1.05$ MHz, corresponding to an internal field of 77.5 G. Figure 5 shows the temperature dependence of σ_1 and σ_2. Again anomalies are revealed at 30 K, but both parameters are practically temperature independent from 60 K up to 110 K (the highest temperature applied), showing no features at T_{cr}. Hence, while ν drops to zero at ~84 K the Gaussian decay continues unchanged, reflecting a field spread of $\Delta B_1=2\ \mu\mathrm{s}^{-1}/\gamma_\mu\simeq 23$ G up to at least 110 K. Finally, Fig. 6 displays the temperature dependence of the amplitudes Ap_1 and Ap_2. As can be seen the oscillating signal becomes dominant at the lowest T and starts to drop above T_{cr}. The Ap_i seem to reflect the population of the two μ^+ fractions producing the two components.

As pointed out above, the ZF signal becomes complex below 18 K. As an example Fig. 7 shows $AP(t)$ at 10 K. It can be fitted with four components, three of them showing Gaussian-damped oscillations corresponding to precession frequencies (internal fields) of 3.0 MHz (221 G), 6.7 MHz (494 G), and 32 MHz (2.36 kG), the fourth showing only an exponential decay with a decay rate of $0.7\mu\ \mathrm{s}^{-1}$, not drastically larger than λ found above 18 K. The width of the three precessing components are 47, 18.8, and 293 G, respectively. The fractional width $\Delta B_i/B_i$ is rather large and may be consistent with the claimed incommensurate AF structure. More

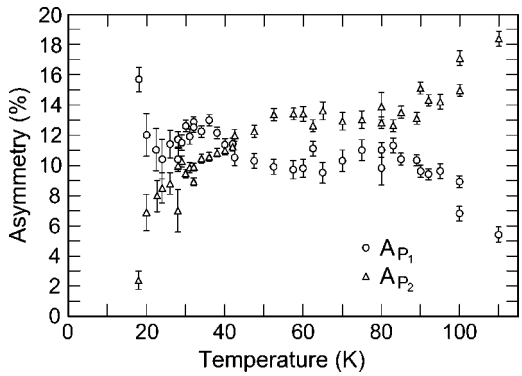

FIG. 6. The temperature dependence of the amplitudes (asymmetries) Ap_1 and Ap_2. Note that the total asymmetry decreases below 30 K. This is due to an increasing non-negligible contribution from the exponentially decaying third component as a result of a not perfect orientation $\boldsymbol{P}(0)\|a$ axis (see caption of Fig. 2).

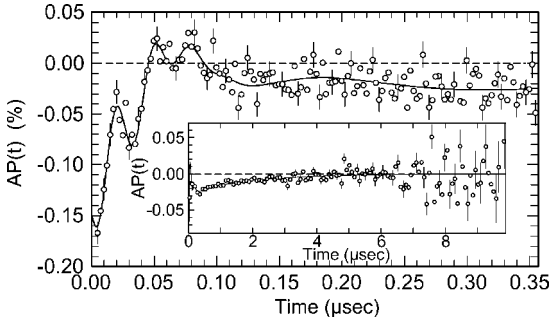

FIG. 7. The zero field signal $AP(t)$ at 10 K ("forward" e^+ detector). The solid line is a fit of a four-component signal as described in the text. The inset shows the signal at long times.

details cannot, at present, be extracted from the data below 18 *K*, which therefore will not be discussed further.

Preliminary TF measurement at 6 kOe produce also two components. The extracted Knight shifts show an orientation dependence which imply that the μ^+ can principally only be located at the sites 2*b*, 2*c*, 2*d*, 2*f*, 4*h* (see Fig. 1), none of which can be excluded on the basis of these rather limited Knight shift data. The TF data are also in other respects quite different from the ZF results (e.g., regarding amplitudes) and do not show anomalous features at 30 K and 84 K. Further systematic TF measurements on single crystals will have to provide the missing information.

IV. DISCUSSION

The results show that the observed spontaneous internal fields are confined to the (b,c) plane for both components. Specifically, for one fraction of μ^+ the average field is different from zero, and for the other fraction it vanishes. What is the origin of the spontaneous fields? It is clear that the underlying structure must be quite different from the modulated antiferromagnetic structure below 17 K as a comparison of Figs. 2 and 7 clearly indicates. The appearance of spontaneous fields above T_N is reminiscent of similar observations in $PrCu_2$.[12] However, while the temperature dependence of the spontaneous field in $PrCu_2$ is quite unusual, reflecting the strain susceptibility $\chi_{xy}(T)$,[13] in the present case $\nu(T)$ for $T \leqslant 30$ K exhibits a classical mean-field behavior with the exponent $\beta = 0.5$. In the former case it was conjectured that the observed magnetic order is driven by a quadrupolar mechanism; in the present case the magnetic order is probably of a more conventional origin, but peculiar in the sense that it was not visible in the neutron scattering work and the new transition temperatures at 30 K and 84 K are not reflected in other bulk parameters, such as the susceptibility and the specific heat.

We have also to understand the unexpected temperature *independence* of the large σ_1 and σ_2 above ~60 K. The latter suggests that there could be a further transition at higher temperatures, which we failed to see so far. The size and isotropy of σ_1 and σ_2 and the anisotropy of p_1 and p_2 exclude that the σ_i originate from randomly oriented Pr-, Co-, and Al-nuclear dipole-fields, i.e., are given by Van Vleck second-moment expressions.[14] Rather the anisotropy of the p_i implies that the fields at the μ^+ are not randomly oriented and hence the relevant magnetic moments can also not be randomly oriented. This excludes also that the large σ_i below 110 K reflect enhanced nuclear dipole fields due to a hyperfine induced polarization of the $4f$ ($3d$) electron shells of Pr (or Co), e.g., in $PrNi_5$ this is known to lead to an enhancement factors of ~10 at low T,[15] which should be proportional to the magnetic susceptibility and therefore strongly temperature dependent. However, the σ_i are nearly temperature independent above 60 K. Hence, also the fields above 30 K at the μ^+ must be of electronic origin and one may consider either the Co $3d$ or the Pr $4f$ electrons as the source of the fields. Since the μ^+ sites have not yet been determined and the contribution of contact-hyperfine fields, originating from the conduction electron spin polarization at the μ^+ site, is not known, it is, however, impossible to model a unique magnetic structure that could reproduce our data. The confinement of the spontaneous fields $\boldsymbol{B}_{\mathrm{int},i}$ to the (b,c) plane implies at least that the ordered moments are also confined to the (b,c) plane if the μ^+ are located at the *f* sites, midway between the Pr or Co sites along the *b* axis, which are rather likely sites (see Fig. 1). One can always construct for all the other possible interstitial site near-neighbor spin arrangements which lead to fields in the (b,c) plane. The observation that the $\boldsymbol{B}_{\mathrm{int},i}$ are probably randomly oriented in the (b,c) plane suggests that the magnetic structure may be of the helical (commensurate or incommensurate) type with the axis of the helix oriented parallel to the *a* axis. On the other hand, the wide variation of $|\boldsymbol{B}_{\mathrm{int},i}|$ (typically $\omega/\sigma_1 \simeq 1$) could indicate that the structure is rather imperfect. The nonoscillating component could simply reflect a random arrangement of frozen moments, confined to a plane, a kind of 2D spin glass. This may explain in part why neutron scattering did not reveal the magnetic order above 17 K.

A rough estimate of the possible magnitude of the ordered moments *m* can be made by considering the shortest distance *r* of a Pr or Co ion from the possible interstitial μ^+ sites and the resulting dipole field m/r^3. The distances range from 2.02 Å for the *f* site to 3.83 Å for the *b* site (see Fig. 1) leading to dipole fields between 1.13 and 0.165 kG/μ_B. Scaling these values down to the observed field at 18 K (or 30 K) one arrives at estimates of $(0.06-0.45)\ \mu_B$ [or $(0.036-0.25)\ \mu_B$]. The actual values may be quite different, e.g., also much smaller, since we have neglected the contact-hyperfine fields and the contributions from the other Pr or Co neighbors. Nevertheless, the estimates give an idea of the order of magnitude and, depending on the assumed μ^+ site, allow us to understand why the high-temperature magnetic order was not seen in the neutron diffraction work and that the 30 K and 84 K transitions were not manifest in, e.g., the specific heat data.

Then the question arises which ions, Pr or Co, may carry the high temperature magnetic order. Concerning Pr it is difficult to understand how a small moment can be created out of the $4f$ electron state. This compound is not known to display Kondo behavior. It appears therefore more likely that the Co constituents are responsible and that the Co associated $3d$ bands produce a complex spin-density wave with a small amplitude, barely contributing to the magnetic entropy.

Now the 30 K anomaly has to be considered. As Figs. 4 and 5 show, not only the spontaneous frequency ν but also the relaxation rates σ_1 and σ_2 display a change in behavior at 30 K, in particular σ_2 rises in a similar way as ν. Obviously the magnetic structure undergoes a transition at 30 K without changing the general structure of the μSR signal, i.e., the amplitudes A_i seem to change smoothly across 30 K (Fig. 6). The pronounced increase of ν and σ_2 could point to a change of the spin density wave amplitude. Perhaps the Pr sublattice starts to be involved in preparation for the phase transition at 17 K. But also the transition at ~83 K, as indicated already above, is not the end of the magnetic phase as the persistence of an anisotropic signal and the large σ_1 and σ_2 imply. The magnetic phase diagram of $PrCoAl_4$ seems, therefore, to be characterized by four transition temperatures.

We have no explanation yet for the temperature dependence of the amplitudes A_1 and A_2. Is this reflecting the population of two different sites or does it indicate different magnetic domains? We do not know. Further measurements at different orientations of the crystal will hopefully provide more information, as well as measurements in longitudinal fields.

Finally, one may consider possible μ^+ induced features. However, we do not see how an isolated μ^+ (only one μ^+ resides in the sample at a time) can induce a static, more or less ordered spin arrangement in its vicinity.

V. SUMMARY AND CONCLUSIONS

Our ZF-μSR studies of $PrCoAl_4$ unexpectedly reveal the persistence of magnetic order above the well-characterized modulated antiferromagnetic state below T_N=17 K and reflect further transitions at 30 K, ~83 K, and, presumably, at a still higher temperature. The magnetic order becomes evident by the appearance of static fields confined to the (b,c) plane and probably more or less randomly oriented in that plane. This may point to an incommensurate spiral structure of the involved moments with the axis of the helix oriented parallel to the a axis, or to a truly random order in two dimensions, resembling a spin glass, where the frozen moments are confined to a certain plane. Our ignorance of the μ^+ sites and contact-hyperfine fields precludes at this time a clear picture of the established magnetic structure, but rough estimates point to the possibility that the involved moments are rather small ($\lesssim 0.1\ \mu_B$). This is taken as a possible indication that the high temperature magnetic order is of the spin wave density type and carried by the 3d electron bands derived from the Co sublattice.

Further detailed measurements of the μ^+ Knight shift will hopefully allow us to determine the μ^+ site(s), and further ZF measurements are intended to extend the present data to higher temperatures.

ACKNOWLEDGMENTS

This work has been performed at the Swiss Muon Source ($S\mu S$) of the Paul Scherrer Institut (PSI) and we are grateful to PSI and its Laboratory for Muon Spin Spectroscopy for providing excellent measuring conditions. The authors wish to thank Professor K. H. J. Buschow for stimulating this work and illuminating discussions.

[1] D. Tung and K. H. Buschow, J. Alloys Compd. **291**, 37 (1999).
[2] P. Schobinger-Papamantellos, G. André, J. Rodríguez-Carvajal, O. Moze, W. Kockelmann, L. D. Tung, and K. H. J. Buschow, J. Magn. Magn. Mater. **231**, 162 (2001).
[3] P. Schobinger-Papamantellos, C. Wilkinson, L. D. Tung, K. H. J. Buschow, and G. I. McIntyre, J. Magn. Magn. Mater. **284**, 97 (2004).
[4] L. D. Tung, D. M. Paul, M. R. Lees, P. Schobinger-Papamantellos, and K. H. J. Buschow, J. Magn. Magn. Mater. **281**, 378 (2004).
[5] R. M. Rykhal, O. S. Zarechnyuk, and Ya. P. Yarmolyak, Dopov. Akad. Nauk. Ukr. RSR, Ser. A: Fiz.-Mat. Tekh. Nauki **39**, 265 (1977).
[6] P. Schobinger-Papamantellos, M. Kenzelmann, A. Schenck, F. N. Gygax, K. H. J. Buschow, and C. Ritter, Physica B **349**, 100 (2004).
[7] P. Schobinger-Papamantellos and K. H. J. Buschow, J. Magn. Magn. Mater. **130**, 242 (1994).
[8] See, e.g., A. Schenck and F. N. Gygax, in *Handbook of Magnetic Materials*, edited by K. H. J. Buschow (Elsevier, Amsterdam, 1995), Vol. 9.
[9] C. P. Slichter, *Principles of Magnetic Resonance* (Springer, Berlin, 1990).
[10] A. Schenck, D. Andreica, F. N. Gygax, D. Aoki, and Y. Onuki, Phys. Rev. B **66**, 144404 (2002).
[11] T. Yamazaki, Hyperfine Interact. **6**, 115 (1979).
[12] A. Schenck, F. N. Gygax, and Y. Onuki, Phys. Rev. B **68**, 104422 (2003).
[13] R. Settai, S. Araki, P. Ahmet, M. Abliz, K. Sugiyama, Y. Onuki, T. Goto, H. Mitamura, and T. Goto, J. Phys. Soc. Jpn. **67**, 636 (1998).
[14] A. Schenck, *Muon Spin Rotation Spectroscopy* (Adam Hilger, Bristol, 1985).
[15] N. Kaplan, D. Ll. Williams, and A. Grayevsky, Phys. Rev. B **21**, 899 (1980).